Thermomechanic behavior of epitaxial GeTe ferroelectric films on Si(111)

Boris Croes, Fabien Cheynis, Michaël Texier, Pierre Müller, Stefano Curiotto, Frédéric Leroy

Thermomechanic behavior of epitaxial GeTe ferroelectric films

Boris Croes,[1,2] Fabien Cheynis,[1] Michaël Texier,[3] Pierre Müller,[1] Stefano Curiotto,[1] and Frédéric Leroy[1]

[1] *Aix Marseille Univ, CNRS, CINAM, AMUTECH, Marseille, France*
[2] *Université de Strasbourg, CNRS, Institut de Physique et Chimie des Matériaux de Strasbourg, Strasbourg, 67000, France*
[3] *Aix Marseille Univ, Univ Toulon, IM2NP, AMUTECH, CNRS, F-13397 Marseille 20, France*

(Dated: October 19, 2023)

A key development towards new electronic devices integrating memory and processing capabilities could be based on the electric control of the spin texture of charge carriers in semiconductors. In that respect GeTe has been recently recognized as a promising ferroelectric Rashba semiconductor, with giant spin splitting of the band structure, due to the inversion symmetry breaking arising from the ferroelectric polarization. Here we address the temperature dependence of the ferroelectric structure of GeTe thin film grown on Si(111). We demonstrate the hysteretic behaviour of the ferroelectric domain density upon heating/cooling cycles by low energy electron microscopy. This behaviour is associated with an abnormal evolution of the GeTe lattice parameter as shown by x-ray diffraction. We explain these thermomechanical phenomena by a large difference of thermal expansion coefficients between the film and the substrate and to the pinning of the GeTe/Si interface. The accumulated elastic energy by the GeTe thin film during sample cooling is released by the formation of a-nanodomains with in-plane ferroelectric polarization component.

I. INTRODUCTION

Due to their use as functional materials, ferroelectric thin films are the subject of extensive research. The discovery of complex ferroelectric polarization textures, e.g. vortices [1 and 2], flux-closure polar domains [3–5] and even skyrmions [6] have attracted lots of attention in ferroelectric materials. These structures occur due to the combined effects of interfacial stress induced by the substrate and to the electrostatic and mechanical boundary conditions at ferroelectric domain walls. The control of such structures is achievable thanks to the ability to synthesize ferroelectric thin films of high crystalline quality and low roughness, using Frank-Van der Merwe growth mode (layer-by-layer growth) and strain engineering methods [7 and 8]. When a single crystalline thin film is grown epitaxially on a substrate at a given temperature, an elastic energy can be stored in the film due to the difference of lattice parameter between the film and substrate materials. This stress can be released during growth, provided that atomic rearrangements at the interface are sufficiently promoted, for instance via the formation of misfit dislocations at the film/substrate interface. When growth is terminated and the sample cooled down, an additional stress may occur: a thermal stress arising from the difference of thermal expansion coefficients between the film and substrate. This stress imposed to the film can be huge and provides the driving force for many stress relief mechanisms such as cracks, buckling or delamination [9]. In the context of thin films exhibiting ferroelastic properties combined with ferroelectricity (multiferroic), the domain structure can be deeply affected.

Ferroelectric Rashba semiconductors are a novel class of materials with strong potential for spintronic applications [10]. On α-GeTe thin films, important results have been achieved. Ferroelectric polarization has been shown to reverse in an electric field [11], and the band structure spin chirality has been consistently changed [12 and 13]. In addition, nonreciprocal charge transport behaviour up to room temperature has been demonstrated in α-GeTe [14]. All these results take advantage of the ferroelectric property of the material. α-GeTe phase has a rhombohedral structure (space group R3m) and bulk Curie temperature well above RT ($T_c \sim 480 - 530$°C). The spontaneous polarization of α-GeTe is along the pseudocubic $< 111 >_{pc}$ leading to the potential formation of four ferroelastic variants (*pc* stands for pseudo-cubic coordinates) and height ferroelectric states. As reported by Wang et al. [15] α-GeTe thin films can be grown with a quasi-single crystalline quality on Si(111) by molecular beam epitaxy using a pre-growth of one monolayer of Sb onto the substrate. Despite a significant lattice mismatch of ∼8.5% with the substrate, the GeTe layer grown at high enough temperature is relaxed since the very beginning of growth. However Croes et al. [16] have shown that GeTe thin films thicker than 30 nm, cooled down to room temperature after growth, have a multiple domain structure with all four ferroelastic variants. The main domain has a ferroelectric polarization perpendicular to the surface plane, *i.e.* in the $[111]_{pc}$ direction, and is called c-domain. The three other ferroelectric domains are called hereafter a-domains with a polarization vector pointing at 19° out of the plane of the film and form 71°-type domain walls with the c-domain. These walls ensure mechanical compatibility and neutrality of the interface between a- and c-domains. Despite the precise morphology and structural characterization of the domains, the driving force responsible for their formation has been overlooked. These studies are a prerequisite for the controlled switching of ferroelectric domains and the understanding of aging properties. Indeed the upward or downward switching of the polarization state of the c-domains is still controversial [11, 12, and 17] and may use a path that passes through the formation of intermediate a-domains. In order to study the energetics of a-domains

formation we have studied micrometer-thick GeTe films where a-domains are well developed. Even though such thick films are not relevant for spintronics due to a nanometric spin diffusion length, the precise determination of the energetic cost associated with polarization switching is crucial for future applications.

In this article we address the hysteretic behaviour of ferroelastic domains in GeTe thin films during temperature cycling. Using low energy electron microscopy (LEEM) we show that ferroelastic a-domains decay continuously when the temperature increases until their complete disappearance at T$\sim$210°C. By cooling the sample they reappear abruptly via a nucleation process with a temperature offset of 30-60°C. The hysteresis of the ferroelastic domain density with respect to temperature is also highlighted in the behaviour of the lattice parameter of GeTe as measured by x-ray diffraction. Indeed, we show that the c-domain exhibits an abnormal thermal expansion behaviour above the temperature of disappearance of the ferroelastic a-domains. We associate this behaviour to the interface pinning of GeTe c-domains with the Si substrate that cannot accommodate the differential of thermal expansion coefficients. The induced thermomechanical stress makes the GeTe thin film in tension when cooling the sample. The estimated elastic energy stored by the GeTe thin film per surface unit for a typical 1 μm-thick film is about 0.5 J/m^2. The stress relief process occurs via the formation of ferroelastic a-domains.

II. EXPERIMENTAL METHOD

Si(111) wafers (Siltronix; 550 μm -thick; ρ=1-10 Ωcm) are first cleaned by acetone and ethanol rinsing before introduction in ultra-high vacuum (UHV, 10^{-8} Pa). Then the substrates are degassed at 730 °C during 12 h followed by repeated high temperature annealing (1250 °C) during a few minutes in order to obtain a clean 7×7 surface reconstruction. First one monolayer of Sb is grown on the Si(111) surface [18], forming the so-called Si(111)-$\sqrt{3}\times\sqrt{3}$-Sb reconstruction that greatly improves the crystalline quality of the GeTe film [15]. The GeTe thin films are grown by co-evaporation of Ge (1175 °C) and Te (310 °C) in UHV on a sample maintained at $\sim$ 260°C. In these conditions the flux ratio between Ge:Te is fixed at 2:5 in order to compensate the high desorption rate of Te [19]. All the evaporation sources are effusion cells from MBE-Komponenten GmbH. After growth, the samples are transferred under UHV conditions thanks to a homemade transfer suitcase and characterized by LEEM and LEED using a LEEM III microscope (Elmitec GmbH). To detect the presence of ferroelastic inclusions, bright-field LEEM images of the GeTe surface are performed at 26 eV incident electron energy where a high contrast is achieved between the majority domain (c-domain) and the inclusions (a-domains). The internal structure of thick GeTe films (>40 nm) has been studied by x-ray diffraction at BM32 beamline (ESRF) and high resolution-transmission electron microscopy (HR-TEM). X-ray diffraction data have been measured at 18 keV [λ=0.06888 nm] with a beam size of 200×300 μm^2 and collected onto a 2D detector. The data have been converted from the detector coordinates (pixel index) to diffraction angles and then to reciprocal space coordinates. The 3D reciprocal space maps are visualized using the ParaView software. To protect the GeTe surface from contamination during sample transfer to the synchrotron UHV chamber, a Te capping was used. The capping is removed in UHV first by a mild Ar ion bombardment at RT (1 keV, 10 μA) to remove the top most oxidized layers then by annealing at ~ 220 °C to desorb the remaining Te layer. HR-TEM investigations of the GeTe/Si interface were performed along $[1\bar{1}0]$ zone axis using a geometrical aberrations-corrected FEI Titan 80-300 microscope, operating at 200 kV. Spherical aberration coefficient (Cs) was tuned to optimize the imaging conditions. Electron transparent TEM lamellae were extracted from the thin films of GeTe on Si by the lift out method using focused ion beam micromachining (Dual beam FIB, FEI Helios 600 NanoLab).

III. RESULTS AND DISCUSSION

Figure 1(a) shows the surface morphology of a 1450 nm-thick GeTe film grown on Si(111)-$\sqrt{3}\times\sqrt{3}$-Sb. This LEEM image is obtained in bright-field mode selecting the main reflected beam arising from the electrons backscattered by the majority domain (c-domain) where the rhombohedron axis and ferroelectric polarization are perpendicular to the $(111)_{pc}$ surface plane. The surface morphology shows extended flat areas limited by slight depressions. In addition needle-shaped structures cross the surface along $\langle 1\bar{1}0\rangle_{pc}$ direction [see black arrows in Fig. 1(a)]. It has been demonstrated that these structures arise from a-type ferroelastic domains that nucleate and grow during cooling to room temperature of the GeTe thin film [16]. These needles appear with a dark contrast in the LEEM image because the beams reflected from their surface plane are slightly off-specular, i.e. tilted by $\sim 2\times 1.4°$ with respect to the normal to the surface, and are not selected in this bright field image. The reflected beams from the a-domain can be seen on the LEED pattern [see black arrows in Fig. 1(b)]. Considering crystallography, the LEED pattern of the surface has a threefold symmetry as expected for single epitaxy of GeTe thin film on the Si(111) substrate. The deduced preferential epitaxy of the c-domain is such that $\mathrm{GeTe}(111)_{pc}\|\mathrm{Si}(111)$ and $\mathrm{GeTe}[1\bar{1}0]_{pc}\|\mathrm{Si}[1\bar{1}0]$ [15 and 16]. The LEEM observation during thermal treatments shows that each a-domain decays continuously in size during heating, disappears and reappears at the same place abruptly under cooling [see Fig. 1(c)]. This process can be repeated many times. This hysteretic behaviour is quantified by measuring the surface fraction

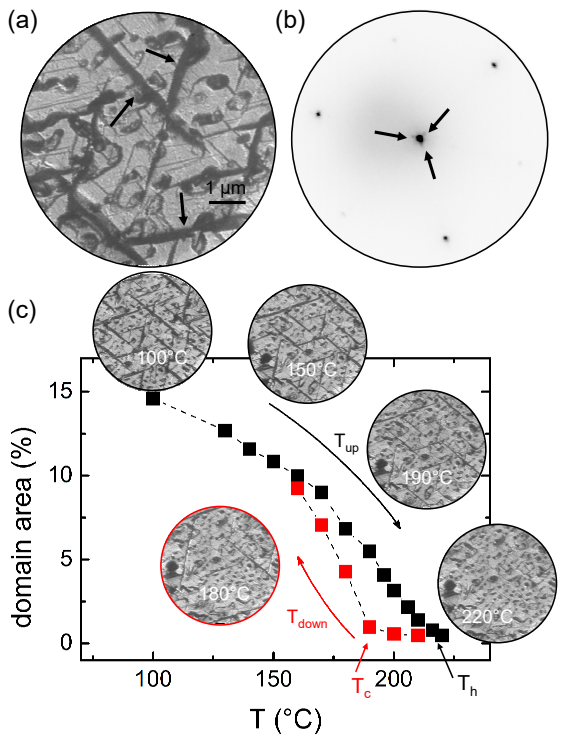

FIG. 1. (a) LEEM image of a GeTe thin film grown on Si(111)-$\sqrt{3} \times \sqrt{3}$-Sb (1450 nm-thick) at 150°C. The black arrows indicates some ferroelastic a-domains. (b) Typical LEED pattern of a GeTe surface at incident electron energy E= 26 eV. The three spots shown by black arrows indicate the reflected beam positions arising from the surface of the ferroelastic a-domains that are slightly tilted with respect to the surface of the c-domain. (c) Plot of the temperature evolution of the fraction of a-domains upon heating (black)/cooling (red). T_h and T_c are respectively the temperature of disappearance (appearance) of a-domains under heating (cooling). Inset: Corresponding LEEM images at different temperatures.

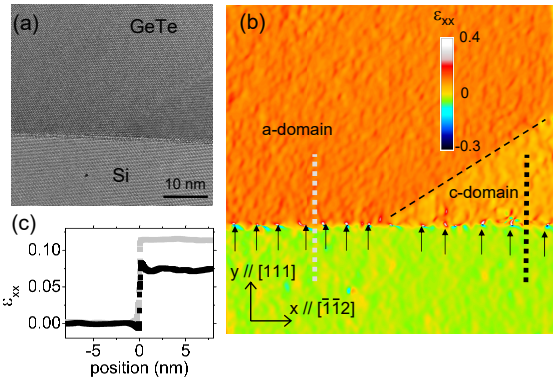

FIG. 2. (a) HRTEM micrograph along $\langle 1\bar{1}0 \rangle_{pc}$ zone axis. (b) Strain field along the interface x-axis (ϵ_{xx}) using GPA method (arrows show misfit dislocations). (c) Profile of ϵ_{xx} along the Si/GeTe interface considering c-domain (black) and a-domain (grey).

of a-domains as function of temperature. Initially, at room temperature, about 15% of the surface is covered with a-domains. This fraction decays continuously upon heating (heating rate 0.3 K/min) until their complete disappearance at $T_h = 220$°C. Upon cooling the a-domains are still absent until $T_c = 190$°C when they nucleate. We recover approximately the same a-domain fraction as during the heating stage at ∼170°C. The thermal hysteresis is $\Delta T = T_h - T_c = 30$ K and is a key parameter of the thermomechanical properties of GeTe thin films grown on Si. The hysteresis indicates that the a-domains need to overpass an energy barrier to nucleate [20].

To address the mechanical state of GeTe thin film at room temperature, the atomic structure of GeTe/Si interface, measured by HR-TEM, shows that it is abrupt and the GeTe layer is fully relaxed [fig. 2(a) and 2(c)]. The in-plane lattice parameter mismatch between the GeTe c-domain and the Si substrate is 7.3±0.2%, i.e. close to the expected value (8.5%) for bulk materials [see fig. 2(b-c)]. It is accommodated by a misfit dislocation network at the GeTe/Si interface. This result is corroborated by in situ RHEED measurements that have shown a relaxed GeTe film since the early stage of growth [21 and 22]. From these observations one could examine the energy gain to switch from c- to a-domain considering the interface with the Si substrate. Comparing qualitatively the interfacial energy cost with Si of both GeTe c-domain and a-domain we can state that (i) the in-plane lattice parameter mismatch is unfavorable for the a-domains since the lattice parameter is ∼11.5% larger than the Si one in the $< 11\bar{2} >_{pc}$ direction [stretching direction, see fig. 2(b-c)] whereas it is ∼7.3% for the c-domains. (ii) The in-plane atomic lattice of the a-domains is also unfavorable considering symmetry since it is monoclinic whereas the atomic lattice is hexagonal for the GeTe c-domains (as for the Si(111) surface). (iii) At last the interface plane of a a-domain is expected to be tilted by 1.4° with respect to the Si surface plane [tilt angle of $(111)_{pc}$ plane, see also LEED pattern in fig. 1(b)] whereas the GeTe c-domain and the Si substrate are coplanar [23]. Therefore switching from c- to a-domain appears to be energetically unfavorable. This qualitative analysis is corroborated by the crystalline structure of GeTe thin film during and after growth since it shows a single c-domain configuration. However, given that cooling causes a-domain formation, we can infer that an additional driving force is involved: the thermomechanical stress induced by the difference of thermal expansion coefficients of Si and GeTe materials.

To address this hypothesis and unravel the mechanisms responsible for the occurrence of ferroelastic a-domains in GeTe thin films and the hysteretic behaviour of the fraction of a-domains as function of temperature, we have performed 3D reciprocal space map measurements by x-ray diffraction during thermal heating under ultra high vacuum. Figure 3(a) shows a series of iso-intensity maps around the symmetric GeTe 222_{pc} Bragg peak at increasing temperature. The map shows

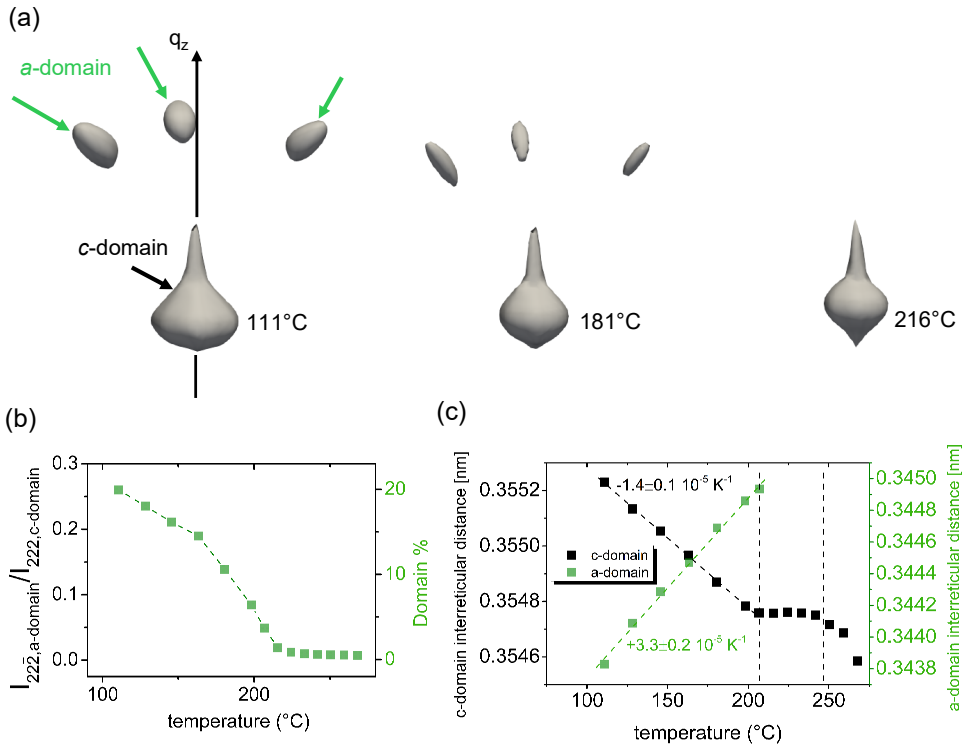

FIG. 3. (a) Series of iso-intensity maps (2000 counts) around 222_{pc} Bragg peak of GeTe thin film (420 nm-thick) at increasing temperature (see complete movie in supplementary materials S1 [24]). The majority c-domain Bragg peak is located at the lower wave vector. Above this main peak, that is stable under annealing, three additional Bragg peaks arising from a-domain inclusions are measured. (b) Plot of the a-domain fraction as function of temperature from the ratio of the integrated intensity of 222_{pc} Bragg peaks arising from the a-domains and the c-domains. (c) Plot of the of GeTe interreticular distance of the c- and a-domains as function of temperature. In the linear range of thermal expansion we deduce the linear expansion coefficients of the c- and a-domains. The dashed vertical lines indicate the range of temperature of the abnormal evolution of the interreticular distance in the c-domain.

four Bragg peaks, one associated with the majority c-domain at lower wave number and three Bragg peaks associated with the three variants of a-domains at higher wave number. The a-domains Bragg peaks are slightly tilted with respect to the specular rod as already described by LEED [see fig. 1(b)]. As the temperature increases, the a-domains Bragg peaks intensity decays monotonously. The decrease of the integrated intensity of the Bragg peaks of the a-domains indicates a volume reduction [fig. 3(b)] and a complete disappearance at 210°C. The a-domain volume fraction is estimated from the ratio of the integrated intensities of the $22\bar{2}_{pc}$ Bragg peaks of the a-domains and 222_{pc} Bragg peak of the c-domains. Both intensities are calculated from the structure factors of the ferroelectric rhombohedral unit cell of GeTe and assuming a displacement of 0.03 nm of the Ge atom with respect to the center of the unit cell of Te atoms. The displacement is along the main axis of the rhombohedron [25]. In the meantime the position of the c- and a-domains Bragg peaks evolve under heating. The temperature evolution of the out-of-plane lattice parameter is deduced from the position, in reciprocal space, of the barycenter of the c- and a-domains Bragg peaks. Initially, at increasing temperature and up to ∼200°, all four Bragg peaks of GeTe (c- and a-domains) converge towards each other. This behaviour is expected since the rhombohedron unit cell of the α-GeTe phase, that is ferroelectric/ferroelastic, relaxes progressively towards the face centered cubic phase that is paraelectric. Therefore the intereticular distance between GeTe$(111)_{pc}$ planes of the c-domain and GeTe$(11\bar{1})_{pc}$ planes of the a-domains get closer. We measure that the GeTe$(111)_{pc}$ interreticular distance of c-domains decreases monotonously [fig. 3(c)] and the associated linear expansion coefficient is negative -1.4±0.1 10^{-5} K^{-1}. In the meantime, the interreticular distance associated to the a-domains, i.e. between GeTe$(11\bar{1})_{pc}$ planes increases. The measured linear expansion coefficient is +3.3±0.2 10^{-5} K^{-1} [fig. 3(c)] and is close to previous measurements [26]. However above 210°C, i.e. when the a-domains have all switched to c-domains, the $(111)_{pc}$ interreticular distance of c-domains stops decreasing, reaches a plateau and decreases again above ∼260°C. This abnormal behaviour of quasi-stability of the interreticular distance with respect to temperature indicates that a strong thermo-mechanical stress builds up in a

temperature range between 210°C and 260°C. Both temperatures correspond respectively to the temperature of disappearance of the a-domains and to the growth temperature of the GeTe thin film. We can notice that this abnormal behaviour of the interreticular distance of the c-domain occurs much before the merge of all Bragg peaks, i.e. in a temperature range where GeTe remains in the rhombohedral ferroelectric α-phase. Indeed the explored temperature range during heating is far below the GeTe phase transition temperature rhombohedron↔fcc (ferroelectric↔paraelectric) that is around 400°C [27 and 28]. Therefore we can safely assume that at the growth temperature of GeTe thin film (260°C), GeTe has a rhombohedral crystal structure with a single domain configuration where the rhombohedron axis is perpendicular to the film surface, i.e. forming a macroscopic c-domain. The a-domains occur only during cooling. This domain switching process in ferroelectrics/ferroelastics is known to be highly sensitive to mechanical stress and this effect may be even more pronounced for epitaxial films. To address the relaxation mechanism prevailing in the formation of these a-domains we infer, from the measured temperature evolution of the interreticular distance in GeTe c-domain, that a thermal stress arises due to the ten times larger linear thermal expansion coefficient of GeTe ($\sim 3.2 \times 10^{-5}$ K^{-1}, [26 and 28]) with respect to Si ($\sim 3.5 \times 10^{-6}$ K^{-1}, [29 and 30]). Assuming that the interfacial misfit dislocations are not enough mobile to accommodate this change [31–34] the lattice parameter contraction of the GeTe film when cooling is hindered by the very low thermal expansion of the Si substrate [fig. 4-(a)-(ii)]. Since the GeTe lattice parameter should decrease during cooling, a tensile in-plane strain occurs in the GeTe layer and a huge amount of elastic energy is stored. The plateau of the interreticular distance of GeTe c-domains in the temperature range of stability of the single c-domain [fig. 3(c)] is a clear indication of the mechanical constraint imposed by the Si substrate. To macroscopically reduce this tensile stress some a-domains nucleate, expanding locally the in-plane lattice parameter in the $\langle 11\bar{2} \rangle$ direction [fig. 4-(a)-(iii)]. The formation of the three variants of a-domains provides a global isotropic in-plane relaxation. When the GeTe layer is annealed again at the growth temperature it recovers its relaxed interface, and therefore the a-domains are elastically useless and spontaneously decay [fig. 4-(a)-(i)]. The hysteretic behaviour of the a-domains indicates that the nucleation energy barrier of a-domains is overpassed when the stored elastic energy is high enough. To estimate the validity of this hypothesis we calculate the stored elastic energy in the GeTe c-domain per surface unit W_{el} under thermal bi-axial strain ϵ_T over the entire layer thickness:

$$W_{el} = 2 \times \frac{Eh}{1-\nu} \epsilon_T^2 = 2 \times \frac{Eh}{1-\nu} \left[\left(\alpha_{GeTe} - \alpha_{Si} \right) \Delta T \right]^2 \quad (1)$$

where $E = 83 \pm 6$ GPa and ν=0.27 are the Young modulus and Poisson ratio [35 and 36], h is the typical film thickness (1 μm), $\alpha_{GeTe,Si}$ are the linear expansion coefficients of GeTe and Si and ΔT is the temperature offset with respect to the relaxed growth temperature (260°C). We can calculate the maximum thermal in-plane strain ϵ_T=0.14 % for ΔT=50° C and the corresponding stored thermoelastic energy per surface unit W_{el} =0.5 J/m^2. This value is consistent with a typical surface/interface energy of a material allowing to create twin domains, e.g. 71°-type domain walls between a- and c-domains [37]. The global strain gain can be estimated from the change of in-plane lattice parameter between c- and a-domain. As shown by Croes et al. [23], the surface lattice of the a-domain is a distorted hexagon [see fig. 4-(b)-(ii)] with a monoclinic unit cell (a_a=b_a=0.429 nm, angle=121.7°) whereas the c-domain has a hexagonal unit cell [a_c=b_c=0.418 nm, angle=120°, see fig. 4-(b)-(i)]. Therefore we can estimate the in-plane strain variation induced by domain switching: $\epsilon = \frac{a_a - a_c}{a_c} = \frac{0.429 \times \cos(58.3/2) - 0.418 \times \cos(60/2)}{0.418 \times \cos(60/2)} = 3.5\%$. Then an equivalent contribution of 4% of a-domains in the GeTe layer provides 3.5% × 4% ∼0.14% extension of the layer that is enough to compensate the accumulated thermal strain at 210°C (ΔT = 50° C). This is indeed what we observe by LEEM at the nucleation of a-domains [see fig. 1-(c)]. As the temperature decreases additional a-domains are continuously formed to reduce

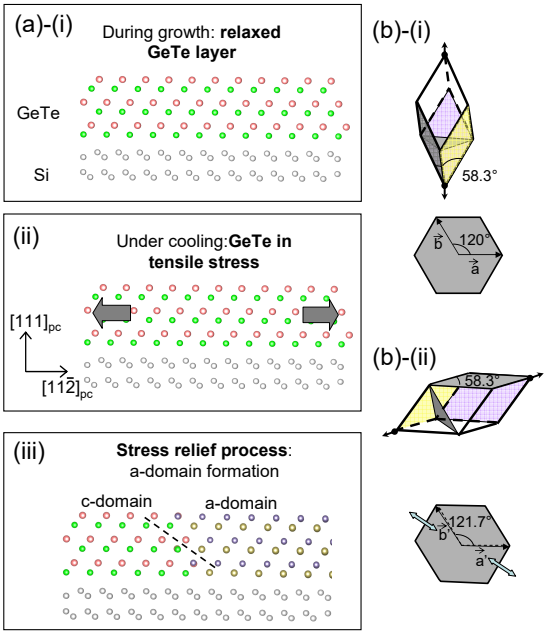

FIG. 4. (a) Scheme of the evolution of the GeTe/Si interface at different stages under thermal treatments: (i) at growth conditions, (ii) after cooling and (iii) after nucleation of a-domain that expands locally the lattice. The change of color of atoms allows to distinguish the c- and a-domains. (b)-(i) Scheme of the rhombohedral crystallographic structure of GeTe c-domain and interface lattice. (b)-(ii) Same as (b)-(i) for a ferroelastic a-domain.

the thermomechanical stress has observed by LEEM and x-ray diffraction.

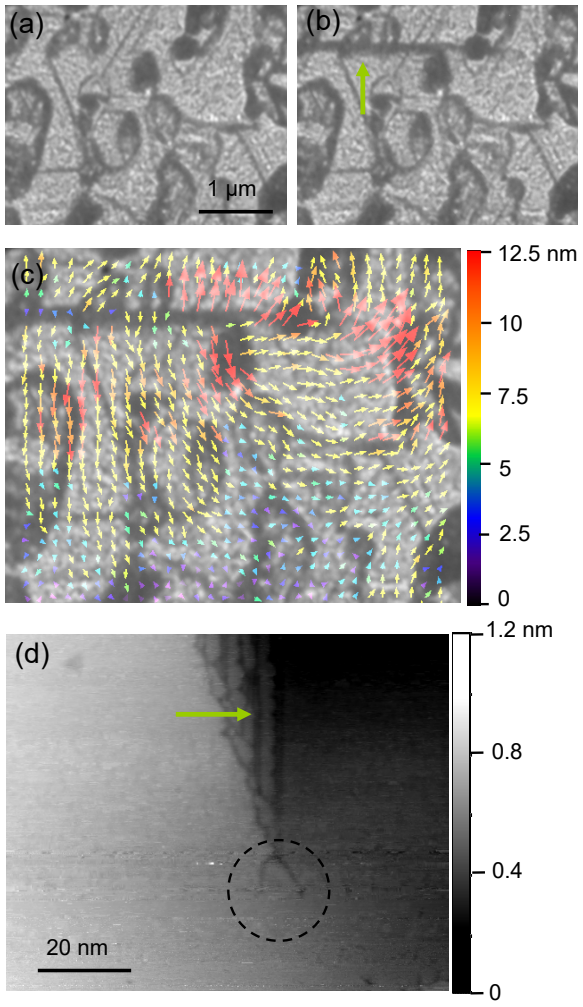

FIG. 5. (a) LEEM image of the GeTe thin film grown just before the nucleation/growth of a a-domain. (b) Same as (a) just after the occurrence of the domain. (c) Superposition of image (b) with the displacement field at the surface. The length and color of the arrows is a measure of the displacement vector (see scale bar). The sudden nucleation of the a-domain generates a shift of the surface of the order of 6 nm (dark areas gives non correct values). (d) STM image at the tip of a a-domain (green arrow). The surface of the a-domain shows complex surface reconstructions as described in ref. [23]. The c-domain close to the tip shows depression lines corresponding to Te vacancies accumulation (dashed circle).

From a local perspective the domain switching process provides a sudden contribution to the stress relaxation. By tracking the occurrence of a-domains during cooling we can measure the displacement field induced by their nucleation at the film surface. Figure 5(a)-(b) shows two LEEM images of the GeTe film surface before and after nucleation of a a-domain (see supplementary material S2 for the movie [24]). The analysis, via image cross-correlation, of the displacement field at the surface induced by the inclusion of a a-domain shows that its occurrence is accompanied by a global displacement of the majority c-domain surrounding the a-domain. This behaviour is characteristic of a nonlinear thermomechanical effect induced by a sudden switch of the ferroelastic state. The observed displacement at the surface of the c-domain close to the central region of the a-domain is d=6±1 nm in the direction perpendicular to the needle. This displacement is observed at each side of the a-domain. Since the width of the a-domain at the surface just after nucleation is W=150±15 nm we can estimate that the relative expansion is $\epsilon = \frac{d}{W} = 2 \times \frac{6}{150}$=8±2%. This value is much larger than the 3.5% linear expansion of the interreticular distance in the $< 11\bar{2} >_{pc}$ direction by switching from c- to a-domain. Therefore the observed displacement of the surface shows that the ferroelastic switching mechanism is part of a more global relaxation process that is also associated with c-domain relaxation that was prevented until the nucleation of the a-domain. In addition the displacement field extracted in the vicinity of the a-domain tip shows an inhomogeneous field. This means that the majority c-domain is inhomogeneously strained in this area. In particular we can expect that the c-domain in front of the tip of a-domain needle may be subject to a large strain field. Figure 5(d) shows a STM image of the surface morphology of a GeTe film close to a a-domain tip. The c-domain is Te-terminated whereas the a-domain shows complex restructuring as described by Croes and coworkers [23]. The STM image shows also slight depressions on the c-domain close the tip of the a-domain (dashed circle). We suspect that these depression lines come from Te advacancies that accumulate locally suggesting possible effect of the local strain field.

IV. CONCLUSION

In conclusion we have studied the thermomechanic behaviour of GeTe epitaxial films on Si(111). At high temperature, i.e. above 210°C GeTe thin films have a single ferroelastic domain configuration called c-domain, where the rhombohedron axis is perpendicular to the surface plane. Below this temperature a-domains, that have an in-plane rhombohedron axis component, nucleate and grow. We have shown that during cooling, the thermal stress induced by the difference of linear thermal expansion coefficients of GeTe and Si is responsible for the formation of these a-domains. We evidence this behaviour via a hysteresis of the a-domain configuration with respect to temperature and by addressing the evolution of the lattice parameter of c- and a-domains under heating using x-ray diffraction. In particular in the c-domain high temperature configuration, the thermal expansion of the GeTe lattice is limited by that of the Si substrate generating a large amount of thermal stress in the film that relaxes via a-domains formation at lower temperature.

V. SUPPLEMENTARY MATERIAL

See the supplementary material S1 for the movie of isointensity maps (2000 counts) around 222_{pc} Bragg peak of GeTe thin film (420 nm-thick) at increasing temperature up to the disappearance of the a-domains. In supplementary material S2 is shown two LEEM images of the GeTe film surface before and after nucleation of a a-domain.

VI. ACKNOWLEDGEMENTS

The project leading to this publication has received funding from Excellence Initiative of Aix-Marseille University A*MIDEX, a french "Investissements d'Avenir" programme through the AMUtech Institute. This work has also been supported by the ANR grants FETh (ANR-22-CE08-0023). We deeply thank Lucio Martinelli for x-ray measurements (Synchrotron ESRF, BM32, Grenoble, France). We thank Martiane Cabié (CP2M, Marseille, France) for lamella preparation of GeTe thin films by FIB.

[1] A. K. Yadav, C. T. Nelson, S. L. Hsu, Z. Hong, J. D. Clarkson, C. M. Schlepueetz, A. R. Damodaran, P. Shafer, E. Arenholz, L. R. Dedon, D. Chen, A. Vishwanath, A. M. Minor, L. Q. Chen, J. F. Scott, L. W. Martin, and R. Ramesh. Observation of polar vortices in oxide superlattices, Nature 530, 198 (2016).

[2] P. Shafer, P. Garcia-Fernandez, P. Aguado-Puente, A. R. Damodaran, A. K. Yadav, C. T. Nelson, S.-L. Hsu, J. C. Wojdel, J. Iniguez, L. W. Martin, E. Arenholz, J. Junquera, and R. Ramesh, Emergent chirality in the electric polarization texture of titanate superlattices, P. Natl. Acad. Sci. USA 115, 915, (2018).

[3] A. Gruverman, D. Wu, H-J Fan, I. Vrejoiu, M. Alexe, R. J. Harrison, and J. F. Scott, Vortex ferroelectric domains, J. Phys.: Condens. Matter. 20, 342201 (2008).

[4] N. Balke, B. Winchester, W. Ren, Y. H. Chu, A. N. Morozovska, E. A. Eliseev, M. Huijben, R. K. Vasudevan, P. Maksymovych, J. Britson, S. Jesse, I. Kornev, R. Ramesh, L. Bellaiche, L. Q. Chen, and S. V. Kalinin, Enhanced electric conductivity at ferroelectric vortex cores in BiFeO3, Nat. Phys. 8, 81 (2012).

[5] Y. L. Tang, Y. L. Zhu, X. L. Ma, A. Y. Borisevich, A. N. Morozovska, E. A. Eliseev, W. Y. Wang, Y. J. Wang, Y. B. Xu, Z. D. Zhang, and S. J. Pennycook, Observation of a periodic array of flux-closure quadrants in strained ferroelectric PbTiO3 films, Science 348, 547 (2015).

[6] S. Das, Y. L. Tang, Z. Hong, M. A. P. Goncalves, M. R. McCarter, C. Klewe, K. X. Nguyen, F. Gomez-Ortiz, P. Shafer, E. Arenholz, V. A. Stoica, S. L. Hsu, B. Wang, C. Ophus, J. F. Liu, C. T. Nelson, S. Saremi, B. Prasad, A. B. Mei, D. G. Schlom, J. Iniguez, P. Garcia-Fernandez, D. A. Muller, L. Q. Chen, J. Junquera, L. W. Martin, and R. Ramesh, Observation of room-temperature polar skyrmions, Nature 568, 368 (2019).

[7] R. Kern, G. Le Lay and J. J. Metois, Current topics in materials Science (ed E. Kaldis) vol. 3 (1979) North-Holland Publishing Co. p. 130.

[8] A. Biswas, C.-H. Yang, R. Ramesh and Y.H. Jeong, Atomically flat single terminated oxide substrate surfaces, Prog. Surf. Sci. 92, 117 (2017)

[9] G. Abadias, E. Chason, J. Keckes, M. Sebastiani, G. B. Thompson, E. Barthel, G. L. Doll, C. E. Murray, C. H. Stoessel, L. Martinu, Review Article: Stress in thin films and coatings: Current status, challenges, and prospects, J. Vac. Sci. Technol. A 36, 020801 (2018).

[10] D. Di Sante, P. Barone, R. Bertacco, and S. Picozzi, Electric Control of the Giant Rashba Effect in Bulk GeTe, Adv. Mater. 25, 509 (2013).

[11] A. V. Kolobov, D. J. Kim, A. Giussani, P. Fons, J. Tominaga, R. Calarco, and A. Gruverman, Ferroelectric switching in epitaxial GeTe films, APL Mater. 2, 066101 (2014).

[12] C. Rinaldi, S. Varotto, M. Asa, J. Slawinska, J. Fujii, G. Vinai, S. Cecchi, D. Di Sante, R. Calarco, I. Vobornik, G. Panaccione, S. Picozzi, and R. Bertacco, Ferroelectric Control of the Spin Texture in GeTe, Nano Lett. 18, 2751 (2018).

[13] J. Krempasky, S. Muff, J. Minar, N. Pilet, M. Fanciulli, A. P. Weber, E. B. Guedes, M. Caputo, E. Mueller, V. V. Volobuev, M. Gmitra, C. A. F. Vaz, V Scagnoli, G. Springholz, and J. H. Dil, Operando Imaging of All-Electric Spin Texture Manipulation in Ferroelectric and Multiferroic Rashba Semiconductors, Phys. Rev. X 8, 021067 (2018).

[14] Y. Li, Y. Li, P. Li, B. Fang, X. Yang, Y. Wen, D.-X. Zheng, C.-H. Zhang, X. He, A. Manchon, Z.-H. Cheng, and X.-X. Zhang, Nonreciprocal charge transport up to room temperature in bulk Rashba semiconductor alpha-GeTe, Nat. Commun. 12, 540 (2021).

[15] R. Wang, J. E. Boschker, E. Bruyer, D. Di Sante, S. Picozzi, K. Perumal, A. Giussani, H. Riechert, and R. Calarco, Toward Truly Single Crystalline GeTe Films: The Relevance of the Substrate Surface, J. Phys. Chem. C 118, 29724 (2014).

[16] B. Croes, F. Cheynis, Y. Zhang, C. Voulot, K. D. Dorkenoo, S. Cherifi-Hertel, C. Mocuta, M. Texier, T. Cornelius, O. Thomas, M.-I. Richard, P. Müller, S. Curiotto, and F. Leroy, Ferroelectric nanodomains in epitaxial GeTe thin films, Phys. Rev. Mater. 5, 124415 (2021).

[17] K. Jeong, H. Lee, C. Lee, L.H. Wook, H. Kim, E. Lee, M.-H. Cho, Ferroelectric switching in GeTe through rotation of lone-pair electrons by Electric field-driven phase transition, Applied Materials Today 24, 101122 (2021).

[18] H. Guesmi, L. Lapena, A. Ranguis, P. MÏller, and G. Tréglia, Sb/Si(111) adsorption:: Hidden phase transitions behind langmuir-like isotherms, Phys. Rev. Lett. 94, 076101 (2005).

[19] K. Perumal, *Epitaxial growth of Ge-Sb-Te based phase change materials.* PhD thesis, Humboldt-Universität zu Berlin, Mathematisch-Naturwissenschaftliche Fakultät I (2013).

[20] M. Kamlah Ferroelectric and ferroelastic piezoceramics - modeling of electromechanical hysteresis phenomena, Continuum Mech. Thermodyn. 13, 219 (2001).

[21] B. Croes, F. Cheynis, Y. Fagot-Revurat, P. Müller, S. Curiotto, and F. Leroy, Early-stage growth of GeTe on Si(111)-Sb, Phys. Rev. Mater. 7, 014409 (2023).

[22] R. Wang, D. Campi, M. Bernasconi, J. Momand, B. J. Kooi, M. A. Verheijen, M. Wuttig, and R. Calarco, Ordered Peierls distortion prevented at growth onset of GeTe ultra-thin films, Sci. Rep. 6, 32895 (2016).

[23] B. Croes, F. Cheynis, P. Müller, S. Curiotto, and F. Leroy, Polar surface of ferroelectric nanodomains in GeTe thin films, Phys. Rev. Mater. 6, 064407 (2022).

[24] See supplemental material at [publisher]. S1: Movie of isointensity maps (2000 counts) around 222_{pc} Bragg peak of GeTe thin film (420 nm-thick) at increasing temperature. The Bragg peaks of a-domains clearly shift to lower wave number and decay with temperature. S2: LEEM movie of the switching process. Image size: $3{\times}3$ μm^2.

[25] D. Kriegner, G. Springholz, C. Richter, N. Filet, E. Mueller, M. Capron, H. Berger, V. Holy, J. H. Dil, and J. Krempasky, Ferroelectric Self-Poling in GeTe Films and Crystals, Crystals 9, 335 (2019)

[26] M. Gallard, M. S. Amara, M. Putero, N. Burle, C. Guichet, S. Escoubas, M.-I. Richard, C. Mocuta, R. R. Chahine, M. Bernard, P. Kowalczyk, P. Noe, and O. Thomas, New insights into thermomechanical behavior of GeTe thin films during crystallization, Acta Materiala 191, 60 (2020).

[27] A. Schlieper, Y. Feutelais, S.G. Fries, B. Legendre, and R. Blachnik, Thermodynamic evaluation of the germanium-tellurium system, CALPHAD 23, 1 (1999).

[28] T. Chattopadhyay, J. X. Boucherle, and H. G. Von Schnering, Neutron diffraction study on the structural phase transition in GeTe, J. Phys. C: Solid State Phys. 20, 1431 (1987).

[29] R. R Reeber and K. Wang, Thermal expansion and lattice parameters of group IV semiconductors, Mater. Chem. Phys. 46, 259 (1996).

[30] H. Watanabe, N. Yamada, and M. Okaji, Linear thermal expansion coefficient of silicon from 293 to 1000 K, Int. J. Thermophys. 25, 221 (2004).

[31] N. A. Pertsev and A. G. Zembilgotov, Domain populations in epitaxial ferroelectric thin films: Theoretical calculations and comparison with experiment, J. Appl. Phys. 80, 6401 (1996).

[32] K. S. Lee and S. Baik, Reciprocal space mapping of phase transformation in epitaxial PbTiO3 thin films using synchrotron x-ray diffraction, J. Appl. Phys. 85, 1995 (1999).

[33] K. Lee, K.S. Lee, and S. Baik, Finite element analysis of domain structures in epitaxial PbTiO3 thin films, J. Appl. Phys. 90, 6327 (2001).

[34] K. S. Lee, J. H. Choi, J. Y. Lee, and S. Baik, Domain formation in epitaxial Pb(Zr,Ti)O-3 thin films, J. Appl. Phys. 90, 4095 (2001).

[35] G. M. Guttmann and Y. Gelbstein, Mechanical properties of thermoelectric materials for practical applications, In Patricia Aranguren, editor, *Bringing Thermoelectricity into Reality*, chapter 4. IntechOpen, Rijeka (2018).

[36] U. E. Ali, G. Modi, R. Agarwal, and H. Bhaskaran, Real-time nanomechanical property modulation as a framework for tunable nems, Nature Comm. 13, 1464 (2022).

[37] A. P. Sutton, R. W. Balluffi, On geometric criteria for low interfacial energy, Acta Metallurgica 35, 2177 (1987).